Am. J. Hum. Genet. 48:911–925, 1991

A Detailed Multipoint Map of Human Chromosome 4 Provides Evidence for Linkage Heterogeneity and Position-specific Recombination Rates

Kenneth H. Buetow,* Rita Shiang,† Ping Yang,* Yusuke Nakamura,‡ G. Mark Lathrop,‡ Raymond White,‡ John J. Wasmuth,§ Stephen Wood,‖ Laura D. Berdahl,† Nancy J. Leysens,† Timothy M. Ritty,† Molly E. Wise,† and Jeffrey C. Murray†

*Division of Population Science, Fox Chase Cancer Center, Philadelphia; †Department of Pediatrics, University of Iowa, Iowa City; ‡ Howard Hughes Medical Institute, University of Utah Health Sciences Center, Salt Lake City; §Department of Biological Chemistry, University of California, Irvine; and ‖Department of Medical Genetics, University of British Columbia

Summary

Utilizing the CEPH reference panel and genotypic data for 53 markers, we have constructed a 20-locus multipoint genetic map of human chromosome 4. New RFLPs are reported for four loci. The map integrates a high-resolution genetic map of 4p16 into a continuous map extending to 4q31 and an unlinked cluster of three loci at 4q35. The 20 linked markers form a continuous linkage group of 152 cM in males and 202 cM in females. Likely genetic locations are provided for 25 polymorphic anonymous sequences and 28 gene-specific RFLPs. The map was constructed employing the LINKAGE and CRIMAP computational methodologies to build the multipoint map via a stepwise algorithm. A detailed 10-point map of the 4p16 region constructed from the CEPH panel provides evidence for heterogeneity in the linkage maps constructed from families segregating for Huntington disease (HD). It additionally provides evidence for position-specific recombination frequencies in the telomeric region of 4p.

Introduction

As a consequence of the search for the gene for Huntington Disease (HD) (Gusella et al. 1983), human chromosome 4 has been the focus of extensive genetic and physical mapping initiatives (Pohl et al. 1988; Whaley et al. 1988; Bates et al. 1989; Pritchard et al. 1989; Snell et al. 1989*b;* Weber et al. 1989; Bucan et al. 1990). These efforts, however, have focused largely on the most telomeric region (4p16), leaving the remainder of the chromosome less well characterized. To date, only coarse genetic maps of the entire chromosome have been constructed. The first multipoint map of the chromosome, produced by Keats (1981) contained five loci. The more recent map of Donis-Keller et al. (1987) contains 19 RFLP-based markers defining 11 unique locations on the chromosome. However, only three of these 19 markers represent known coding sequences; vitamin D binding protein (GC), alcohol dehydrogenase (ADH3), and the MN and Ss red cell antigens now defined by their genes, glycophorin A (GYPA) and glycophorin B (GYPB), respectively.

We previously reported an 11-point map (Murray et al. 1988) that spans 4p11 to 4q31. Presented here is an extension of that map that details the meiotic mapping results for 53 loci whose genetic location spans the length of human chromosome 4. Three maps are presented: (1) a 20-locus anchor map spanning 4pter-4q31 which contains nine loci detecting variation in or near coding sequences, (2) likely locations for 32 additional loci (19 gene probes, 13 anonymous probes) demonstrating significant linkage to loci on chromosome 4, and (3) a detailed genetic map of 10 loci in the 4p16 region.

Received August 24, 1990; revision received January 8, 1991.

Address for correspondence and reprints: Kenneth H. Buetow, Ph.D., Fox Chase Cancer Center, 7701 Burholme Avenue, Philadelphia, PA 19111.

0002-9297/91/4805-0010$02.00

Material and Methods

Polymorphisms

RFLPs previously reported in the literature or detected in this study were used as shown in table 1. Sources and descriptions of probes are available in the primary references listed and through the Human Gene Mapping (GDB) Library at Johns Hopkins University. Data for GC (protein variants) and MNS (blood group variants) were supplied by CEPH (Centre d'Étude du Polymorphisme Humain). Searches for new RFLPs were made using DNA from 7–10 unrelated Caucasians and digested with 8–66 restriction enzymes with different specificities. RFLPs were then substantiated using family studies and tests for Hardy-Weinberg equilibria. Only standard Southern blots were used in this analysis so that polymorphisms involving DNA fragment sites outside 500–25,000 bp or fragment-site differences of less than 50–1,000 bp (depending on parent size band) would not have been detected. Polymorphism data were managed utilizing computer software provided by CEPH. The typing data utilized in this report have been submitted to CEPH for distribution in public data bases.

Study Population

The multipoint gene map was constructed utilizing the CEPH reference pedigree panel (Dausset et al. 1990). This panel consists of 40 families (31 nuclear pedigrees and nine nuclear families) with an average sibship size of 8.3. For a subset of markers, an additional 21 nuclear pedigrees were included in the panel. These families are members of the extended CEPH panel and are described in detail elsewhere (Dausset et al. 1990).

DNA Analysis

RFLP analysis utilized DNA samples provided by CEPH extracted from lymphoblastoid or fibroblast cell lines. Typings for each polymorphic system were performed by standard methods (Murray et al. 1983). In brief, DNA was digested with the appropriate restriction enzyme according to the manufacturer's instructions and electrophoresed on 0.8%–1.2% agarose gels. Transfers were done to Zetabind using the Southern blotting procedure described by the manufacturer (AMF-Cuno). Prehybridization and hybridization were carried out as recommended by the manufacturer. Probes were radiolabeled by the random primer method of Feinberg and Vogelstein (1983, 1989) utilizing (32P)dCTP.

Linkage Analysis

The strategy and methods for primary map construction are well established and have been described in detail elsewhere (Donis-Keller et al. 1987; Lathrop et al. 1988). The map construction procedure used here is summarized below. First, pairwise linkage analysis was performed utilizing the lod score method (Morton 1955) as implemented in the analysis programs LINKAGE (version 4.9) (Lathrop et al. 1984) and CRIMAP (version 2.3) (P. Green, unpublished results). Standard lod tables (univariate and bivariate) were calculated utilizing MLINK and CRIMAP-PAIRS. Maximum-likelihood pairwise recombination estimates were obtained utilizing CLODSCORE and CRIMAP-PAIRS. Likelihood ratio tests were used to evaluate sex differences in recombination.

The linkage information content for each locus was evaluated by estimating the number of meioses in which this marker was potentially informative. In practice, this value was determined by calculating a lod value for each locus under the assumption that it is linked to itself with no recombination. The lod value was converted to equivalent meioses according to the procedure of Edwards (1976).

A group of loci in which one or more loci demonstrated significant pairwise linkage with another was defined as a linkage group. A multipoint map for each linkage group was constructed by the following algorithm. A small subgroup of highly informative loci (large number of equivalent meioses) was selected from the linkage group. The likelihood for all possible orders, assuming sex-averaged interlocus recombination frequencies, was evaluated for these loci utilizing the computer program CRIMAP. The likelihood of all locus orders within 20 log10 likelihood units of the most likely order were then evaluated utilizing the LINKAGE program CILINK. For a single order to be selected over another order, it was required to demonstrate odds of 1,000 to 1 improvement over the next best order by both methods.

Additional loci within the linkage group were added to the skeletal map constructed above by two related methods. In the first method, an algorithm analogous to a stepwise regression algorithm was utilized. First, the likelihood of each new locus in all intervals within the map was evaluated. New loci were considered in the order of their information content. Likelihoods were calculated both by fixing the interlocus recombination values (LINKMAP-CMAP) and by reestimating the values (CRIMAP-BUILD). A locus was determined to have a unique location within the map if

Table 1

RFLPs Utilized in Study

Gene/Locus	Probe(s)	Polymorphic Enzyme(s)	Physical Location	Equivalent No. of Meioses	Reference
ADH3	pAD74	*Xba*I, *Stu*I	4q21-q23	224	Smith et al. 1985
ALB	F47	*Pst*I, *Sac*I, *Eco*RV	4q11-q13	299	Murray et al. 1983
AREG	AR9	*Msp*I, *Taq*I	4q13-q21	160	J. Murray, unpublished data
ATP1BL1	B51-1-4	*Eco*RI, *Kpn*I	4p16-q23	192	Georgiou et al. 1989
D4F26	pBS847	*Taq*I, *Pst*I, *Sca*I	4p16.3	228	Altherr et al. 1989
D4S1	3.6	*Bgl*II	4q11-q21	327	Gilliam et al. 1984
D4S10	G8,PTV20	*Hin*dIII, *Bgl*I, *Bgl*II	4p16.3	518	Gusella et al. 1983; Carlock et al. 1987
D4S12	A1	*Hae*III	4pter-q26	59	Scambler et al. 1985
D4S13	A46	*Msp*I	4pter-q26	147	Gilliam et al. 1984
D4S35	g920	*Msp*I	4p11-q11	330	Dietz et al. 1986
D4S43	Multiple	*Taq*I, *Mcl*I, *Msp*I, *Bgl*I	4p16.3	305	Gilliam et al. 1987*a*; MacDonald et al. 1989
D4S62	p8	*Hin*cII	4p16.2-16.1	125	Hayden et al. 1988
D4S67	pBS8.6	*Hin*dIII, *Taq*I	4p13-q13	207	Wood et al. 1986
D4S90	D5	*Stu*I, *Hin*cII	4p16.3	301	Youngman et al. 1988
D4S95	pBS674	VNTR (*Hin*dIII), *Taq*I	4p16.3	417	Smith et al. 1988
D4S96	pBS678	*Msp*I	4p16.3	357	Smith et al. 1988
D4S98	pBS731	*Sac*I	4p16.3	126	Smith et al. 1988
D4S101[a]	CRI-R227	*Taq*I	4	233	Donis-Keller et al. 1987
D4S111	p157-9	*Pst*I	4p16.3	105	Pohl et al. 1988
D4S115	p252-3	*Hae*III, RsaI	4p16.3	203	Pohl et al. 1988
D4S123	pIBS17	*Taq*I	4pter-q21	240	Berdahl et al. 1988*b*
D4S124	pMCOC14	VNTR (*Pst*I)	4	154	Nakamura et al. 1988*a*
D4S125	pYNZ32	VNTR (*Hae*III), *Bgl*I	4p16.3	401	Nakamura et al. 1988*b*
D4S126	p309	*Sac*I, *Hae*III	4p16.3	308	Richards et al. 1988
D4S144	pIRM19-1	*Hin*dIII, *Pst*I	4	292	This paper
D4S145	LE24	*Taq*I	4	369	This paper
D4S163	EFD139	VNTR (*Hin*cII, *Hin*dIII)	4	350	J. Wasmuth, unpublished data
D4S139	pH30	VNTR (*Hin*cII, *Hin*dIII)	4	520	Milner et al. 1989
D4Z1	Xba-340	*Sac*I	Centromere	72	J. Murray, unpublished data
EGF	EGF121	*Hin*cII, *Sac*I	4q25	195	Ritty and Murray, 1989
ENX2	pens2	*Eco*RI, *Pvu*II	4q25	123	Ritty et al., in press
F11	FXI	*Stu*I, *Sac*I	4q35	75	J. Murray, unpublished data
FBA	pγfib	*Taq*I	4q28	259	Humphries et al. 1984
FBB	pβfib	*Bcl*I	4q28	. . .	Murray et al. 1985
FBG	pγfib	*Kpn*I	4q28	. . .	Murray et al. 1985
FGFB	fgfbe	*Bgl*I	4q25	6	This paper
GC	GC	Protein	4q12-q13	537	Cox et al. 1989
GYPA	MN	Red cell	4q28	496	Cox et al. 1989
GYPB(Ss)	pGPB	*Hin*cII, red cell	4q28-q31	496	J. Murray, unpublished data
HOX7	phox7	*Mbo*II	4p16.1	27	J. Murray, unpublished data
HVBS6	PF19	*Taq*I, *Rsa*I	4q32	191	Pasquinelli et al. 1988
IF	HI-1971	*Bcl*I	4q24-q25	104	Shiang et al. 1989
IL2	IL2-3	*Kpn*I	4q26-q27	30	Murray et al. 1988
IL8	pIL8	*Hin*dIII	4q13-q21	259	Modi et al. 1990
INP10	gIFN31-7	*Bcl*I, *Eco*RI	4q21	295	Murray et al. 1988
KIT	VKIT	*Hin*dII	4p11-q22	117	Berdahl et al. 1988*a*
LPC2A	pNL	*Sac*I	4q21-q31	169	Leysens et al. 1989
MGSA	TC870	*Sca*I	4q21	109	Beck et al. 1989
MLR	MR3750	*Stu*I	4	39	J. Murray, unpublished data
MT2P1	pMT2	*Eco*RI	4p11-q21	371	Murray et al. 1987
PDGFRA	pPDGFRA	*Eco*RI		3	J. Murray, unpublished data
PF4	PF4	*Eco*RI	4q12-q21	83	Guzzo et al. 1987
RAF1P1	RAF2	*Bgl*I	4p16.1	362	Gilliam et al. 1987*b*

[a] Typing provided by Collaborative Research Institute.

alternative locations could be excluded with odds of greater than 1,000 to 1 by either method.

After a new locus was placed, the confidence in the current map was reevaluated. First, the likelihood of all possible orders of nonskeletal loci placed in the same interlocus skeletal map interval was considered. If alternative orders of the nonskeletal loci were not excluded by odds of 1,000 to 1, nonskeletal markers were removed from the interval until this significance level was reached. Loci were removed based on information content (number of meioses), with the least informative loci removed first. This analysis utilized the LINKAGE program CILINK. Next, the likelihood of inversions of adjacent loci for the complete map was evaluated utilizing CRIMAP-FLIPS and CILINK. As before, inversion alternatives within the map with relative odds of less than 1,000 to 1 by either method resulted in removal of a locus. After a new locus was assigned to a map location, all remaining unplaced loci were reevaluated.

The map was also constructed by an alternative method. The skeletal map obtained from all possible order analyses was used as an ordered locus cluster for a CRIMAP BUILD run. This procedure sequentially considers the incorporation of each unplaced locus in an existing map in a manner analogous to step-up multiple regression analysis. All recombination values are reestimated as the test locus is evaluated in each map interval. In constructing this map, a locus was assigned a unique location within the map only if relative odds were 1,000 to 1 in favor of this location over all others.

Finally, after all loci with unique placements were mapped, a final verification procedure was employed. Locus orders obtained from CRIMAP BUILD runs, starting with various two-locus clusters, were evaluated.

Results

RFLPs

New RFLPs detected in this study are presented in table 2. Enzymes, band sizes, and allele frequencies based on unrelated CEPH family members are summarized.

Pairwise Analysis

The chromosome 4 data set consisted of 85 probe/enzyme combinations which identify 53 unique loci. This reduction in systems was due to the fact that, in many instances, multiple RFLPs were detected by the same probe, or multiple probes identified the same genetic location. In these instances, haplotypes were created and utilized in subsequent analyses. Additionally, GYPA and GYPB were haplotyped and considered as a single locus, as were FGA, FGB, and FGG, reducing the total number of loci to 50. Twenty-five of the loci utilized were anonymous DNA segments, while the remaining 28 represent gene-specific probes.

Pairwise linkage analysis indicated that 45 loci constituted a single linkage group (each locus demonstrated significant linkage with one or more loci). An additional three loci (F11, D4S139, and D4S163) formed an unlinked group which maps to 4q35 based on the in situ hybridization location for F11 (Kato et al. 1989). Because of the low number of informative meioses available, two loci, FGFB and PDGFRA, did

Table 2

New RFLPs Detected in This Study

Gene/Locus (Probe), Enzyme, and Allele Size	Allele Frequency	Previously Described Polymorphic Bands
D4S125 (pYNZ32):		
*Bgl*I:		
8 kb	.24	VNTR
5 kb	.21	VNTR
3 kb	.02	VNTR
Other fragments	.54	VNTR
RAF1P1 (raf2):		
*Bgl*I:		
7 kb	.91	13.3 kb, 6.2 kb
4.7 kb	.09	13.3 kb, 6.2 kb
HVBS6 (PF19):		
*Rsa*I:		
1.5 kb	.46	*Taq*I
1.0 kb	.04	*Taq*I
D4S144 (pIFM19-1):		
*Bgl*I:		
10 kb	.30	None
5.8 kb	.70	None
*Pst*I:		
2.4 kb	.69	None
1.7 kb	.31	None
*Rsa*I:		
1.8 kb	.25	None
1.0 kb	.75	None
*Sca*I:		
11 kb	.67	None
7.5 kb	.33	None
*Hin*dIII:		
4.5 kb	.20	None
4.0 kb	.80	None

not demonstrate significant linkage with the other 48 markers. A sex difference in recombination was observed for the majority of pairwise values. However, within the 45-locus linkage group, only 79 of the 990 pairs showed a significant sex difference in recombination by a standard statistical criterion ($\alpha = 0.05$). Those pairs showing a significant sex difference are shown in table 3. Of the 79 pairs, 64 comparisons showed an excess of recombination in females while the remaining 15 pairs demonstrated excess in male recombination. All significant male excess recombination was observed with a marker physically localized to 4p16. Thirteen of the significant female excess values (16%) involved the D4S35 locus, which physically maps near the centromere. When a multiple-comparison adjustment was made to the significance criteria (Hochberg 1988), only one pair (FBA/FBB/FBG and GC) showed a significant sex difference in recombination. This interval, which physically spans the central region of 4q, showed excess female recombination.

Primary Multipoint

The multipoint map was constructed by subdividing the map into two physical clusters: loci within band 4p16 and loci in the 4p12–4q26 region. All possible order analysis was used to determine the order of a subset of the most informative loci within each physical region. D4S10, D4S43, D4S90, D4S95, D4S126, D4S145, and RAF1P1 were used as skeletal loci for the 4p16 cluster. The average number of equivalent meioses in the panel for these seven loci was 368. The 4p12–4q26 skeletal loci consisted of ADH3, ALB, D4S1, D4S35, GC, IL8, INP10, and MT2P1. A total of 292 equivalent meioses, on average, were available for these eight loci.

To be considered unique, the best order had to demonstrate odds of 1,000 times greater than the next most likely order. The orientation of each unique order with respect to each cluster was then evaluated. All possible order orientations for each cluster were evaluated. As before, for an orientation to be considered unique, it was required to demonstrate odds 1,000 times greater than the next most likely orientation.

Five additional loci were added to the 15-point skeletal map described above utilizing the stepwise algorithm. This 20-point unique location map is presented in figure 1. The average interlocus distance in this map is 10 cM (assuming Kosambi-level interference). However, as is evident from figure 1, two regions have a high map density (D4S90-D4S62 and D4S1-INP10). As seen in previous chromosome 4 maps, sex-specific recombination rates vary considerably along the length of the chromosome. Likelihood ratio tests indicate, however, that a sex-averaged map is not significantly less likely than a sex-specific recombination rate map ($\chi^2 = 20.2$, 19 df, $P = .3826$).

Utilizing the location score method (LINKAGE-CMAP), it was possible to determine the one lod support interval for each uniquely placed locus. Support was determined by evaluating the likelihood of the test locus at various map positions within the interval defined by flanking markers. The interval defined by the flanking markers and remaining intervals within the map were held constant. The support interval for each locus is shown in figure 2. The majority of loci, while confidently placed with respect to order, show rather large variation in location within the assigned interval. A total of 30 loci could not be uniquely placed within the multipoint map utilizing strict significance criteria. Likely locations for these markers are shown in figure 3.

4p Multipoint

Long-range restriction maps that contain 10 of the markers utilized in this study have been generated for the 4p16 region of chromosome 4 (Cox et al. 1989; MacDonald et al. 1989; Bucan et al. 1990). These restriction maps consist of three well-characterized regions separated by gaps of indeterminate length. A combination of genetic and physical mapping methods have permitted the derivation of a unique order for these loci (MacDonald et al. 1989).

To permit comparison of these studies with the map results obtained from the CEPH reference panel, five additional loci with assigned physical locations were added to the five loci with unique genetic locations described above. Presented in figure 4 is the physical map of the region presented beside sex-averaged and sex-specific genetic maps of 4p16.3. The meiotic distance encompassed by the flanking markers (D4S10 and D4S90) is 9 cM (5 cM in females, 14 cM in males.)

To determine whether the interlocus distances observed here differed significantly from those estimated in Venezuelan families segregating for the HD locus (MacDonald et al. 1989), likelihood ratio tests contrasting the two maps were made. MacDonald et al. have reported a five-point map of the region consisting of nine loci. Within the five-point map they observed three clusters of physically adjacent loci

Table 3

Statistically Significant Sex-specific Heterogeneity Pairwise Recombination Values

Locus		Sex-averaged Recombination	Sex-specific Recombination		
1	2		Male	Female	χ^2 (1 df)
IL8	D4S67	.15	.04	.26	5.25
IL8	D4S12	.20	.00	.34	4.47
D4S124	IL8	.39	.50	.00	7.92
D4S145	VKIT	.50	.00	.50	5.53
GC	D4S13	.21	.10	.36	6.26
GC	VKIT	.16	.08	.32	5.07
GC	D4S67	.18	.07	.31	6.31
GC	D4S1	.22	.05	.43	6.86
GC	LPC2A	.50	.50	.00	4.14
D4S1	D4S13	.20	.00	.43	8.98
D4S1	D4S1	.15	.00	.28	3.96
D4S1	D4S12	.14	.00	.48	4.79
D4S1	D4S111	.41	.23	.50	4.33
AREG	D4S124	.34	.07	.50	8.34
D4S10	VKIT	.37	.27	.50	4.28
D4S10	D4S145	.31	.23	.42	4.79
D4S90	D4S62	.15	.42	.06	7.64
D4S90	D4S43	.04	.08	.00	6.08
EGF	D4S13	.50	.00	.50	5.53
EGF	D4S67	.34	.24	.50	4.01
EGF	D4S1	.26	.15	.39	4.65
ATP1BL1	D4S13	.06	.11	.00	3.87
ATP1BL1	GC	.19	.11	.28	4.84
FBA/FBG	LPC2A	.22	.13	.50	5.34
FBA/FBG	EGF	.35	.23	.45	4.47
D4S35	VKIT	.06	.00	.14	5.89
D4S35	IL8	.19	.09	.28	6.40
D4S35	GC	.16	.07	.31	20.31
D4S35	AREG	.23	.15	.44	8.75
D4S35	D4S10	.39	.32	.50	6.72
D4S35	D4S90	.44	.33	.50	4.14
D4S35	EGF	.47	.23	.50	9.03
D4S35	FBA/FBG	.37	.29	.50	4.19
INP10	D4S13	.25	.08	.46	11.88
INP10	ATP1BL1	.20	.10	.45	12.94
INP10	D4S35	.20	.13	.33	8.29
GYPA/GYPB	LPC2A	.03	.00	.50	6.26
GYPA/GYPB	F11	.36	.14	.48	4.10
GYPA/GYPB	FBA/FBG	.12	.04	.18	6.22
MT2P1	D4S13	.22	.11	.41	4.28
MT2P1	D4S67	.17	.04	.25	4.70
MT2P1	D4S1	.06	.00	.10	5.80
MT2P1	EGF	.29	.15	.44	4.28
MT2P1	D4S35	.21	.12	.31	5.07
D4S126	D4S62	.05	.15	.00	5.71
D4S126	D4S35	.42	.33	.50	4.61
ADH3	D4S1	.35	.09	.50	5.25
ADH3	AREG	.32	.18	.50	4.47
ADH3	D4S35	.38	.24	.50	7.46
ADH3	MT2P1	.30	.16	.40	4.37
D4S95	D4S62	.18	.50	.03	13.59
D4S95	D4S43	.02	.03	.00	3.96

(*continued*)

Table 3 (continued)

Locus		Sex-averaged Recombination	Sex-specific Recombination		
1	2		Male	Female	χ^2 (1 df)
D4S95	D4S90	.04	.08	.00	8.52
D4S95	D4S35	.47	.32	.50	5.48
D4S96	D4S62	.11	.21	.00	6.95
D4S96	D4S126	.04	.06	.00	5.30
D4S96	D4S95	.04	.08	.00	8.15
D4F26	D4S62	.17	.29	.00	8.66
D4F26	D4S43	.05	.07	.00	4.51
HVBS6	GYPA/GYPB	.15	.05	.30	11.93
D4S123	D4S43	.23	.14	.50	5.80
D4S123	D4S126	.21	.10	.30	4.24
D4S144	D4S124	.18	.00	.38	5.48
D4S125	D4S96	.05	.08	.00	6.03
RAF1P1	D4S10	.18	.12	.23	4.37
RAF1P1	D4S43	.18	.09	.25	4.37
PF4	D4S145	.42	.21	.50	4.61
PF4	GYPB/GYPB	.50	.00	.50	5.53
PF4	D4S123	.41	.00	.50	4.97
PF4	RAF1P1	.25	.00	.49	4.14
ALB	D4S13	.26	.05	.37	7.87
ALB	D4S67	.16	.07	.29	7.00
ALB	D4S43	.37	.30	.50	5.30
ALB	EGF	.27	.19	.40	4.19
ALB	D4S35	.15	.11	.27	5.34
ALB	D4S126	.34	.28	.50	4.10
D4S101	FBA/FBG	.31	.17	.42	6.86
D4S101	GYPA/GYPB	.22	.06	.34	14.09
D4S101	HVBS6	.25	.15	.39	5.66

that showed no recombination with each other (D4S96/D4S111/D4S115, D4S98/D4S113/D4S114, and D4S43/D4S95). Typings for all but the D4S113 and D4S114 loci were available for the CEPH panel. Utilizing the seven remaining loci, a multipoint map for the CEPH data set was estimated. Unlike MacDonald et al.'s findings, recombination was observed within each cluster described above. As such, only the most informative marker in the CEPH data set (D4S96 for the D4S96/D4S111/D4S115 and D4S95 for the D4S43/D4S95 clusters, respectively) was used to define the locus in additional multipoint map comparisons.

A significant difference was observed between the length of the two maps. The contrast of the maximum-likelihood, sex-specific CEPH map versus the likelihood obtained assuming the MacDonald et al. (1989) map distances (all meioses) produced a χ^2 of 21.87 (8 df, $P < .0052$). Whether the difference may have been due to recombination differences on HD-bearing versus non-HD-bearing chromosomes was then tested. First, the pairwise recombination estimates for HD and non-HD chromosomes presented in MacDonald et al. were contrasted to the maximum-likelihood estimates obtained from the CEPH panel (table 4). Utilizing standard significance criteria, six of the 14 CEPH comparisons showed a significantly greater recombination value than the HD-bearing chromosome estimates. Only 1 of 14 comparisons differed when contrasted to non-HD meioses in the MacDonald et al. data set. After adjusting for multiple comparisons, two of the 14 pairwise recombination estimates from the HD meioses were rejected. No non-HD estimates were observed to be significantly different by the revised criteria.

Finally, genetic maps generated using a subset of the 4p16.3 loci for HD and non-HD meioses were compared to the map generated from the CEPH data

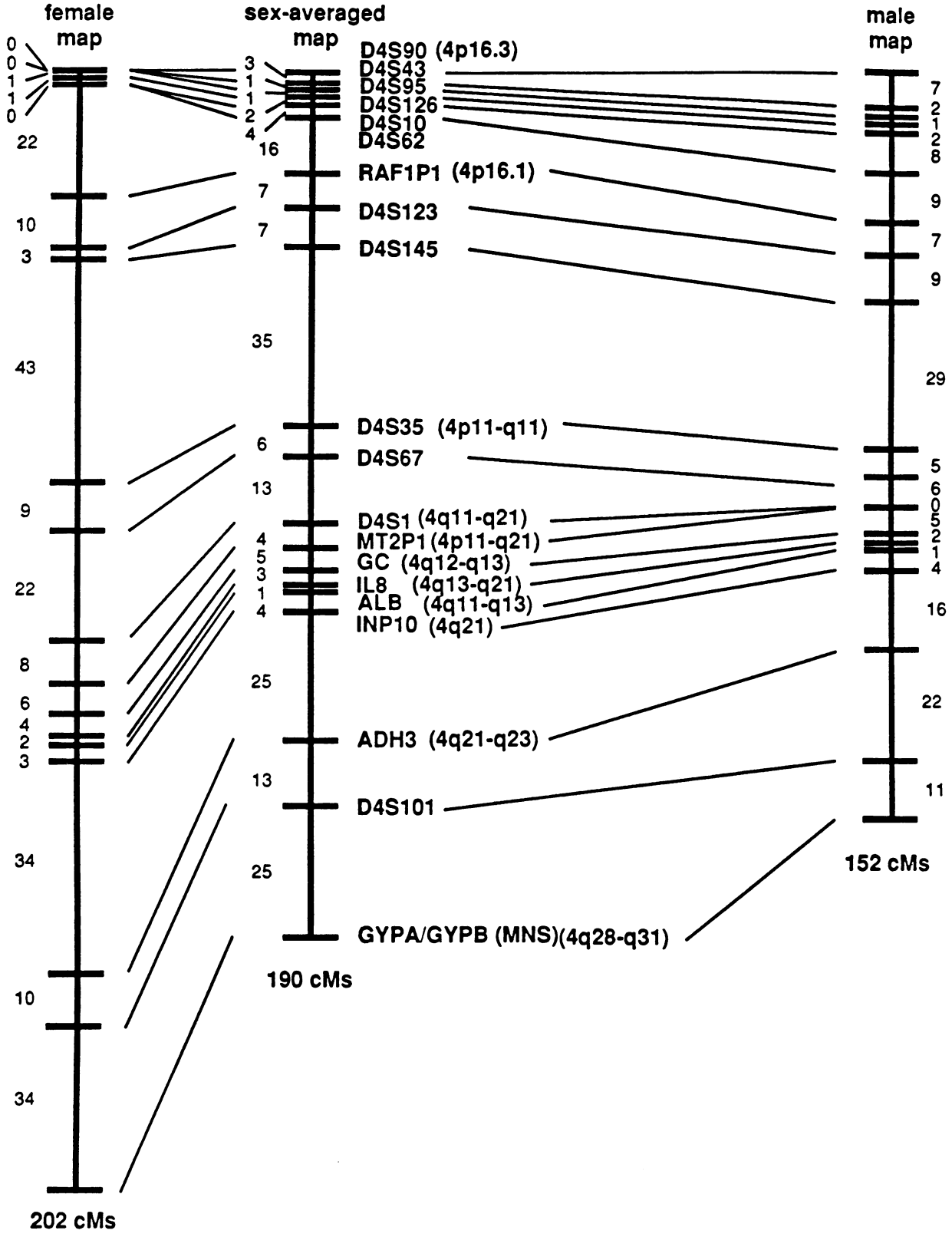

Figure 1 Sex-averaged and sex-specific genetic anchor maps of chromosome 4. Interlocus intervals are presented as map distances (in centimorgans) calculated under the assumption of Kosambi-level interference.

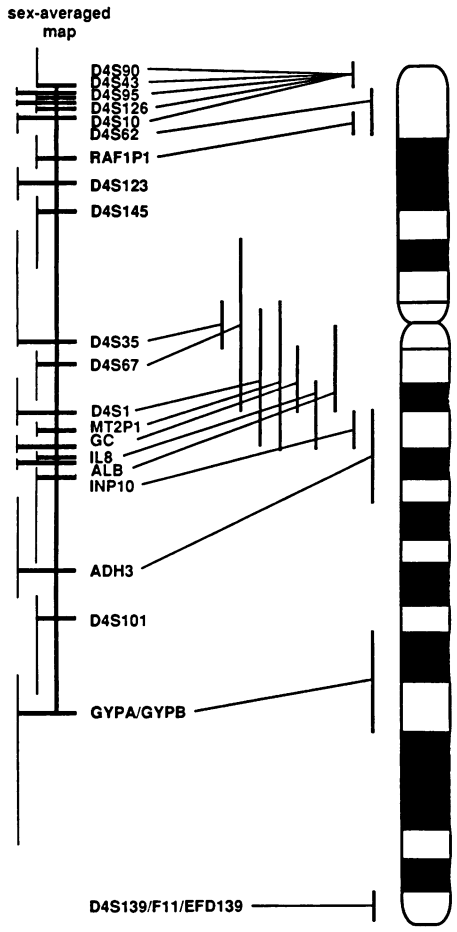

Figure 2 Support interval for each locus within multilocus genetic map. The bracket adjacent to each locus represents the range of likely (within one multilocus lod unit of maximum) alternative locations for each locus within each map interval defined by fixed flanking loci. Brackets adjacent to the chromosome 4 ideogram represent the shortest region of overlap for physical assignments.

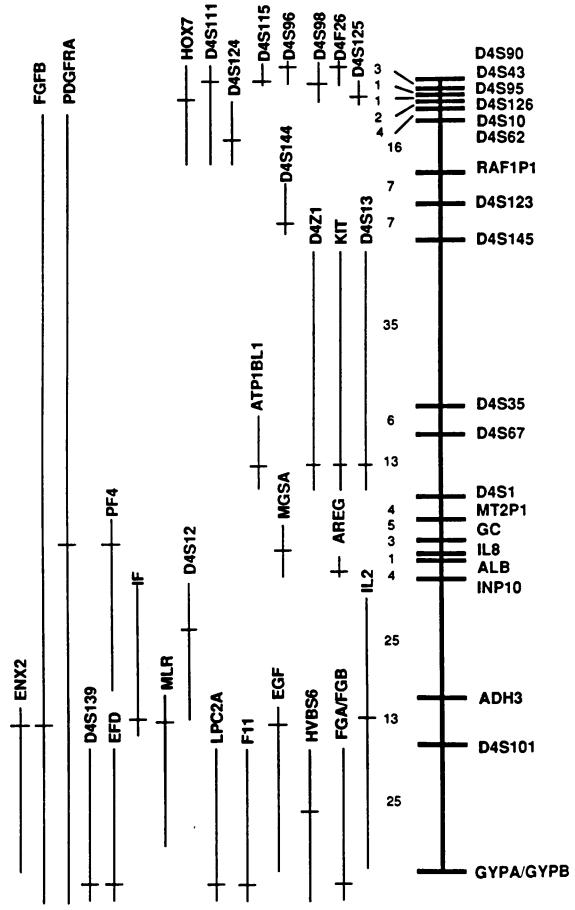

Figure 3 Likely locations for loci which could not be uniquely placed in multilocus map. The cross-bar represents the best location within the multipoint map. The bracket represents alternative map intervals from which the locus could not be excluded with odds of greater than 1,000 to 1.

set. MacDonald et al. (1989) provide HD and non-HD sex-averaged maps for four points: D4S10, D4S95/D4S43, D4S96/D4S115/D4S111, and D4S90. As above, a CEPH data-set map was generated utilizing the most informative locus as the representative of the completely linked cluster. Likelihood contrasts excluded both the HD and non-HD parameter set for the CEPH data set (for non-HD, $\chi^2 = 11.44$, 3 df, $P = .0096$; for HD, $\chi^2 = 33.90$, 3 df, $P < .0001$). However, the non-HD parameter set provided a better overall fit to the data, with 75,358:1 better odds than the HD set.

Relationship of Meiotic and Physical Maps of 4p

Given the current undefined gaps in the physical map, a comprehensive evaluation of the relationship between physical and recombination distance is premature. Nevertheless, several interesting evaluations are possible. Of the estimated 6-Mb distance between D4S90 and D4S10, 2.8 Mb, or 46%, is represented within the three physically mapped clusters. Under the assumption that recombination should be uniformly distributed over all units of physical distance, one recombination unit should equal 1 Mb of physical distance. Given that most of the 6 Mb assumed to be

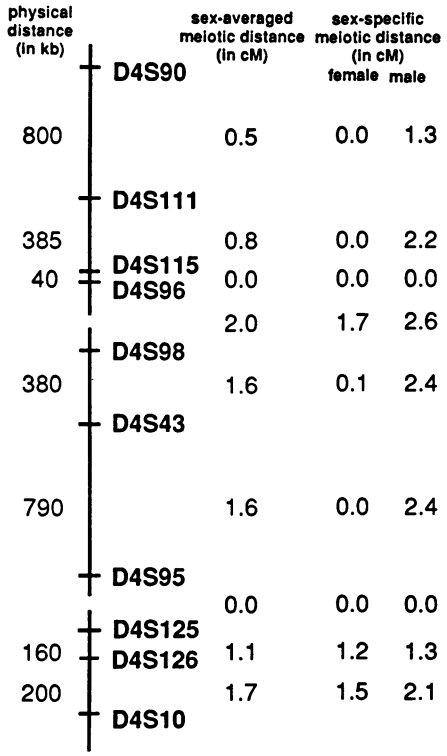

Figure 4 Sex-averaged and sex-specific genetic maps of chromosome 4p16.3. Locus order and physical distances are based on previously reported physical mapping studies (MacDonald et al. 1989). Interlocus intervals are presented as map distances (in centimorgans) calculated under the assumption of Kosambi-level interference. Gaps are not drawn to scale.

contained in 4p16.3 is circumscribed by D4S10 and D4S90, the ratio observed here is 1 cM to 638 kb (1,224 kb in females, 428 kb in males). While its recombination rate is generally higher than the uniform rate, the overall region does not show the gross excess of recombination per physical unit that may have been expected for a telomeric region.

A comparison of interval-specific recombination shows a great deal of variation when compared to physical distance separating points (fig. 4). Most striking among these is the high recombination rate in the D4S10-D4S126 interval. Physical mapping places these loci approximately 200 kb apart, or 3% of the total physical distance in the region. Meiotic mapping places the loci 1.7 cM apart (1.5 in females, 2.1 in males) which constitutes 28% of the total meiotic distance. Comparison of other regions shows average to above-average relationships of recombination to physical distance (fig. 4).

The lack of concordance between meiotic and physical distance estimates may, in part, be explained by the distribution of recombination within 4p16.3. To evaluate this, ratios of meiotic to physical distance with respect to chromosomal location were plotted. Each ratio was assigned a location based on its displacement from D4S10. To estimate the relative position of loci mapped to the middle fragment (the physical fragment bounded by gaps in the Bucan et al. [1990] map), the physical distance accounted for on each fragment was subtracted from the total physical distance assumed to be present in the region. This difference (3,080 kb) was then equally divided and assigned to each gap. Therefore, the most external marker on the middle fragment was assumed to be 1,540 kb from its nearest neighbor on the adjacent fragment. Ratios based on these physical estimates were not included in the analysis. The results of this analysis are presented in figure 5.

Examination of figure 5 showed that the recombination rate observed per unit of physical distance decreased dramatically as one moved closer to the telomere. To test the significance of this relationship, a simple linear regression model was fitted to the sex-averaged recombination/physical distance ratio. A correlation coefficient of $-.93$ ($P = .0022$) was observed between the recombination/physical distance ratio and chromosomal location. Eighty-seven percent of the variance of the ratio was explained by chromosomal location of the interval.

Discussion

Chromosome 4 has long been a focus on human gene–mapping efforts. The localization of the serum marker GC (Mikkelson et al. 1977) and red cell antigen polymorphisms MN and Ss (Bootsma and McAlpine 1979) resulted in chromosome 4 evaluation in many early linkage studies. The mapping of HD to the most distal region of the long arm also brought a concerted effort to find and clone this important gene. RFLP-based maps of the entire chromosome, however, have been less comprehensive than those for the 4p region.

We present here a detailed map of chromosome 4. It represents an integration of a detailed map of the 4p16.3 region with ordered markers forming a continuous linkage group spanning to 4q31. In addition to a 20-point primary map, likely locations for an additional 30 loci are presented. Among the 50 mapped loci, 19 points represent known coding sequences. Included among these loci are genes that may be im-

Table 4

Comparison of Pairwise Recombination Estimates from 4p16.3 Genetic Maps

Comparison	CEPH Maximum-Likelihood Estimate	MacDonald et al. (1989) HD Meioses Pairwise Recombination Estimate	HD Meioses χ^2 (1 df)	Non-HD Meioses Pairwise Recombination Estimate	Non-HD Meioses χ^2 (1 df)
D4S10-D4S43	.052	.022	7.04*	.040	.81
D4S10-D4S95	.034	.022	1.58	.040	.27
D4S10-D4S90	.059	.030	9.82*	.060	1.92
D4S43-D4S96	.034	.008	5.55*	.013	2.80
D4S43-D4S111	.025	.008	2.71	.013	1.01
D4S43-D4S115	.015	.008	.32	.013	.02
D4S43-D4S90	.033	.008	8.05*	.022	1.10
D4S95-D4S96.....	.040	.008	9.96*	.013	5.56*
D4S95-D4S111	.008	.008	.00	.013	.26
D4S95-D4S115	.022	.008	.73	.013	.22
D4S95-D4S90	.009	.008	.00	.022	.01
D4S96-D4S90	.009	.001	2.61	.008	.01
D4S115-D4S90	.011	.001	2.89	.008	.07
D4S111-D4S90	.024	.001	4.43*	.008	.86

* $P < .05$.

portant in cardiovascular disease (FGA/FGB) or cancer (KIT, EGF, IL2, HVBS6), or are candidates for a variety of other human diseases.

The map presented here is comparable with previous maps generated for subregions of chromosome 4. The large excess of female recombination near the centromere observed by Donis-Keller et al. (1987) is also observed here. The sex-averaged map distances observed between GC and MNSs (GYPA/GPYB), the largest definable region of overlap between this map and the current map, are also very similar. Donis-Keller et al. (1987) observed 79 cM (assuming Kosambi interference) between GC and MNS, whereas 78 cM are observed in our study. A priori, one would expect these maps to be largely similar. Both the Donis-Keller et al. and current map utilized the CEPH reference panel and CEPH provided typing for GC and MNS. Additionally, two loci within the interval were also common to both maps (ADH 3 and D4S101), although laboratory specific typings were used to characterize ADH3.

The same was not true when the 4p16 map con-

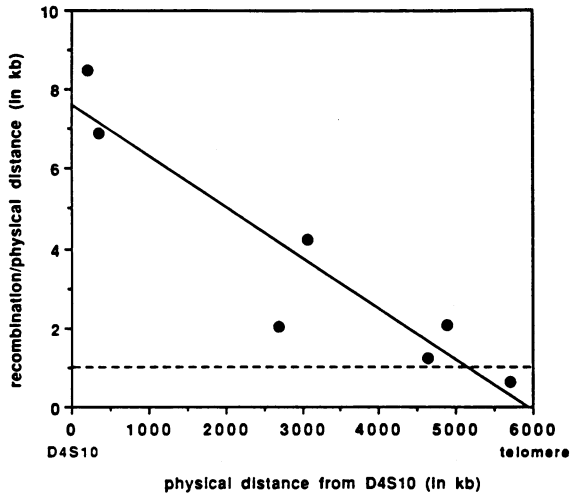

Figure 5 Relationship of chromosomal position to recombination per physical distance unit. Location is measured as physical distance (in kilobases) from D4S10. Recombination values were initially expressed as map units. The solid line represents expected values predicted by a linear model explaining recombination per physical distance unit as a function of location. The dashed line shows expected values under the assumption of a uniform rate.

structed here was compared to that generated utilizing Venezuelan pedigrees segregating for HD (MacDonald et al. 1989). While both maps demonstrated greater male than female sex-specific recombination rates, the CEPH map was also significantly longer than the HD-based map. The most striking region of discrepancy is in the region surrounding D4S43. In the MacDonald et al. (1989) map, D4S43 and D4S95 are not separated by recombination. In the CEPH data set these markers are separated by 1.6 cM. Similarly, the more proximal markers D4S111 and D4S115 are separated by 0.8 cM in the CEPH data but show no recombination in the Venezuelan data. It is not possible to conclusively compare the observed differences in the absence of variance estimates or raw data for the HD pedigrees. For example, one possible source of difference is differential male and female contributions to the CEPH and Venezuelan sex-averaged maps. However, the observation that the CEPH pairwise recombination estimates do not differ significantly from those obtained from non-HD meioses by MacDonald et al. (1989) supports the possibility of linkage heterogeneity in this region of 4p16.3. Further support is provided by the observation that the better-fitting multipoint parameter set is the one composed of the non-HD recombination values by odds greater than 10,000 to 1. A definitive answer will not be possible until both data sets are jointly evaluated. Such an analysis is necessary to incorporate variation inherent in both sets of recombination estimates.

Linkage heterogeneity in 4p16.3 may provide an explanation for several of the provocative observations associated with the efforts to locate the HD gene. Obligate recombination events observed in families segregating for HD have resulted in inconsistent localizations of the gene (Cox et al. 1989). In one collection of families (Doggett et al. 1989; Robbins et al. 1989; Skraastad et al. 1989), HD is localized to the most distal 325 kb of 4p16.3. This location is telomeric to the most distal marker in the map presented here, D4S90. Alternatively, MacDonald et al. (1989) and Snell et al. (1989*b*) find evidence that HD is proximal to D4S90. Support for this localization additionally comes from the observation of linkage disequilibrium between the more proximal markers D4S95 and D4S98 (Snell et al. 1989*a*; Theilman et al. 1989). A reduced region of recombination for HD-bearing chromosomes may account for the observed linkage disequilibrium between HD and markers in its vicinity. The low recombination and linkage disequilibrium could be due to a microinversion in 4p16.3 in HD patients. Such a small inversion might suppress local recombination (Szauter 1984). As physical maps of the region have been generally created utilizing cell lines from non-HD patients (Bucan et al. 1990), an inversion, as yet, may have gone undetected. Such an inversion could explain the discrepancies in map location for HD linkage disequilibrium and reduced recombination.

Historically, human gene mapping has been more of a beneficiary than contributor to knowledge of recombination and genetic structure of genomes. However, with the increasing level of resolution of human gene maps, this situation is changing. This is best illustrated by the examination here of the relationship between recombination rates and physical location. As a consequence of the efforts to localize the gene for HD, nearly the entire p16.3 band of chromosome 4 has been physically mapped. Cloning of the 4p telomere (Doggett et al. 1989) now allows the placing of a definitive endpoint on both the physical and genetic maps of 4p. As such, it is possible to examine the pattern of recombination near telomeres of mammalian chromosomes.

Cytogenetic studies of chiasma have shown a disproportionate number of events to be located near the telomeres of chromosomes (Hulten 1974). It has never been known whether this distribution was due to terminalization of chiasma from recombination events that had occurred more proximally, or represented evidence for high telomere recombination rates per unit of physical distance. Evidence is presented here that the latter is true. The 4p16.3 region shows, on average, 32% greater recombination than expected, given the estimated DNA content of the band. Moreover, the D4S10-D4S126 interval shows an 8.5-fold excess recombination rate for the 200-kb interval of physical distance. Hulten (1974) finds up to 60-fold variation in chiasma distribution over the lengths of chromosomes. This value is dramatically higher than the proportions observed in this small portion of one single human chromosome.

Hulten (1974) also showed a higher number of chiasmata in 4p at diakinesis in males than in females. Alternatively, Bojko (1985) showed that crossing-over was proportionately greater in females than in males in the last 5% (approximately 10 million bp) of chromosome 4p. Our data show an increase in recombination in the penultimate 5–10 million bp (from RAF1P1 to D4S62) for females as well as males, but this reverses itself in the last two million bp (D4S95-D4S90) where male recombination is greater than fe-

male. This short region represents only 1% of the physical length of the chromosome, and the discrepancy with the data of Bojko may represent the inability of her cytogenetic techniques to resolve this region.

Perhaps more interesting is the observed relationship between physical location and recombination rate. It is well known from mapping studies in experimental organisms that recombination varies with cytogenetic location. In *Drosophila melanogaster* (DM), Charles (1938) showed that recombination rate per cytogenetic unit increases as the telomere is approached. The increase peaks, however, prior to reaching the end of the chromosome. In the remaining 12% of the cytogenetic length of the DM X chromosome, recombination drops dramatically. Physical mapping studies of D4S10 place it in the range of 80% of the cytogenetic length of the short arm from the centromere. Consistent with the DM findings, the highest rate of recombination per physical unit is observed with respect to D4S10. As in Charles's study, this rate falls in a linear manner as the telomere is approached. However, unlike Charles, researchers can now make use of accurate estimates of DNA content in each interlocus interval. This permits unequivocal demonstration that the declining rate is not due to reduced target DNA in each interval. Whether D4S10 represents the peak for 4p awaits further physical mapping studies proximal to the locus. In humans, several studies have implicated telomeres as preferential sites of recombination. VNTR sequences cluster in telomeres (Royle et al. 1988) and are associated with chiasmata (Chandley and Mitchell 1988). Chromosome 4p contains several VNTR sequences. The recent identification of a DNA-binding protein for tandem repeats (Collick and Jeffreys 1990) will allow for additional structure-function studies of VNTRs and telomeres in recombination.

Acknowledgments

We thank P. Green for providing the CRIMAP program. Probes utilized in this study were generously provided by J. Arriza (MLR), G. Bell (EGF), P. Besmer (KIT), D. Bowen-Pope (PDGFRA), C. Brechot (HVBS6), E. Davie (FBA, FBB, FBG, F11), M. Fukuda (GYPA, GYPB), G. Gilliam (D4S35), J. Gusella (pXP500, C4H, pKP1.65, S7, S4, G8, 157–9, 252–3, P309), G. Goldberger (IF), T. Hulsebos (D4Z1), J. Iddes (FGFB), M. Jaye (ENX2), R. Lawn (ALB), K. Matsushima (IL8), E. Milner (D4S139), G. Plowman (AREG), F. Ramirez (HOX7), J. Ravetch (INP10), R. Sager (MGSA), M. Schull (ATP1BL1), D. Shaw (D4S90), M. Smith (ADH3), and B. Wallner (LPC2A). Probes for D4S10, D4S35, ALB, ADH3, D4S123, D4S144, MT2P1, EGF, D4S62, RAF1P1, and D4S163 are available through the ATCC. This work is supported in part by USPHS grants CA47816, CA06927, and RR05895 (K.W.B.); and HD20998, GM07031, and GM40864 (J.C.M.) from the National Institutes of Health and by an appropriation from the Commonwealth of Pennsylvania.

References

Altherr MR, Smith B, MacDonald ME, Hall L, Wasmuth JJ (1989) Intrinsic polymorphism of variable number of tandem repeat loci in the human genome. Nucleic Acids Res 16:8487–8496

Bates G, Baxendale S, Sedlacek Z, Poustka A-M, Youngman S, MacDonald M, Whaley WL, et al (1989) A telomere clone likely to contain the mutant form of the Huntington's disease locus. Cytogenet Cel Genet 51:959

Beck JS, Sager R, Murray JC (1989) A ScaI RFLP for the GRO gene on chromosome 4. Nucleic Acids Res 17:8895

Berdahl LD, Murray JC, Besmer P (1988*a*) A *Hin*dIII RFLP demonstrated for the kit oncogene on chromosome 4. Nucleic Acids Res 16:4740

Berdahl LD, Smith RF, Murray JC, Buetow KH (1988*b*) A *Taq*I RFLP demonstrated for pIBS17 (D4S123), a single copy sequence on chromosome 4. Nucleic Acids Res 16: 2743

Bojko M (1985) Human meiosis IX: crossing over and chiasma formation in oocytes. Carlsberg Res Commun 50: 43–72

Bootsma D, McAlpine P (1979) Report of the committee on the genetic constitution of chromosomes 2, 3, 4, and 5. Cytogenet Cell Genet 25:21–31

Bucan M, Zimmer M, Whaley WL, Poustka A, Youngman S, Allitto BA, Ormondroyd E, et al (1990) Physical maps of 4p16.3, the area expected to contain the Huntington disease mutation. Genomics 6:1–15

Carlock LR, Vo TD, DeHaven CR, Murray JC (1987) An anonymous genomic clone that detects a frequent RFLP adjacent to the D4S10 (G8) marker and Huntington's disease. Nucleic Acids Res 15:377

Chandley AC, Mitchell AR (1988) Hypervariable minisatellite regions are sites for crossing-over at meiosis in man. Cytogenet Cell Genet 48:152–155

Charles DR (1938) The spatial distribution of crossovers in X-chromosome tetrads of Drosophila melanogaster. J Genet 36:103–126

Collick A, Jeffreys AJ (1990) Detection of a novel minisatellite-specific DNA-binding protein. Nucleic Acids Res 18:625–629

Cox DR, Murray JC, Buetow KH (1989) Report of the committee on the genetic constitution of chromosome 4. Cytogenet Cell Genet 51:121–136

Dausset J, Cann H, Cohen D, Lathrop M, Lalouel J, White R (1990) Centre d'Etude du Polymorphisme Humain

(CEPH): collaborative genetic mapping of the human genome. Genomics 6:575–577

Dietz JN, Robbins T, Cannon LA, Schwartz CE, Carey JC, Johnson JP, Kivlin J, Skolnick MH (1986) Linkage analysis of von Recklinghausen neurofibromatosis: chromosomes 4 and 19. Genet Epidemiol 3:313–321

Doggett NA, Cheng J-F, Smith CL, Cantor CR (1989) The Huntington disease locus is most likely within 325 kilobases of the chromosome 4p telomere. Proc Natl Acad Sci USA 86:10011–10014

Donis-Keller H, Green P, Helms C, Cartenhour S, Weiffenbach B, Stephens K, Keith TP, et al. (1987) A genetic linkage map of the human genome. Cell 51:319–337

Edwards JH (1976) The interpretation of lod scores in linkage analysis. Cytogenet Cell Genet 16:289–293

Feinberg AP, Vogelstein B (1983) A technique for radiolabelling DNA restriction endonuclease fragments to high specific activity. Biochemistry 132:6–13

——— (1984) A technique for radiolabelling DNA restriction endonuclease fragments to high specific activity: addenum. Anal Biochem 137:266–267

Georgiou C, Shull M, Lane LK, Lingrel JB, Murray JC (1989) RFLPs for ATP1BL1 on chromosome 4. Nucleic Acids Res 17:8894

Gilliam TC, Bucan M, MacDonald ME, Zimmer M, Haines JL, Cheng SV, Pohl TM, et al (1987*a*) A DNA segment encoding two genes very tightly linked to Huntington's disease. Science 238:950–952

Gilliam TC, Scambler P, Robbins T, Ingle C, Williamson R, Davis KE (1984) The positions of three restriction fragment length polymorphisms on chromosome 4 relative to known genetic markers. Hum Genet 68:154–158

Gilliam TC, Tanzi RE, Haines JL, Bonner TI, Faryniarz AG, Hobbs WJ, MacDonald ME, et al (1987*b*) Localization of the Huntington's disease gene to a small segment of chromosome 4 flanked by D4S10 and the telomere. Cell 50:565–571

Gusella J, Wexler N, Conneally PM, Naylor S, Anderson M, Tanzi R, Watkins P, et al (1983) A polymorphic DNA marker genetically linked to Huntington's disease. Nature 306:234–238

Guzzo C, Wiener M, Rappaport E, LaRocco P, Surrey S, Poncz M, Schwartz E (1987) An *Eco*RI polymorphism of a human platelet factor 4 (PF4) gene. Nucleic Acids Res 15:380

Hayden MR, Hewitt J, Wasmuth JJ, Kastelein JJ, Langlois S, Conneally M, Haines J, et al (1988) A polymorphic DNA marker that represents a conserved expressed sequence in the region of the Huntington disease gene. Am J Hum Genet 42:125–131

Hochberg Y (1988) A sharper Bonferroni procedure for multiple tests of significance. Biometrika 75:800–802

Hulten M (1974) Chiasma distribution at diakinesis in the normal human male. Hereditas 76:55–78

Humphries SE, Iman AMA, Robbins TP, Cook M, Carritt B, Ingle C, Williamson R (1984) The identification of a DNA polymorphism of the alpha fibrinogen gene and the regional assignment of the human fibrinogen genes to 4q2t-qter. Hum Genet 68:148–153

Kato A, Asakai R, Davie EW, Aoki N (1989) Factor XT (F11) is located on the distal end of the long arm of chromosome 4. Cytogenet Cell Genet 52:77–78

Keats BJB (1981) Linkage chromosome mapping in man. University Press of Hawaii, Honolulu

Lathrop GM, Lalouel JM, Julier C, Ott J (1984) Strategies for multilocus linkage analysis in humans. Proc Natl Acad Sci USA 81:3443–3446

Lathrop GM, Nakamura Y, Cartwright P, O'Connell P, Leppert M, Jones C, Tateishi H, et al (1988) A primary genetic map of markers for human chromosome 10. Genomics 2:157–164

Leysens NJ, Newkirk NG, Murray JC (1989) SacIXbaI polymorphisms detected by lipocortin 2A (LPC2A). Nucleic Acids Res 17:5417

MacDonald ME, Haines JL, Zimmer M, Cheng SV, Youngman S, Whaley WL, Wexler N, et al. (1989) Recombination events suggest potential sites for the Huntington's disease gene. Neuron 3:183–190

Mikkelson M, Jacobsen P, Henningsen K (1977) Possible localization of Gc-system on chromosome 4: loss of long arm 4 material associated with father-child incompatibility within the Gc-system. Hum Hered 27:105–107

Milner ECB, Lotshaw CL, Willems van Dijk K, Charmley P, Concannon P, Schroeder HW (1989) Isolation and mapping of a polymorphic DNA sequence pH30 on chromosome 4 (D4S139). Nucleic Acids Res 17:4002

Modi WS, Dean M, Seuanez H, Makaida N, Matsushima K, O'Brien SJ (1990) Monocyte-derived neutrophil chemotactic factor (MDNCF/IL-8) resides in a gene cluster along with several other members of the platelet factor 4 gene superfamily. Hum Genet 84:185–187

Morton NE (1955) Sequential tests for the detection of linkage. Am J Hum Genet 7:277–318

Murray JC, Buetow K, Chung D, Aschbacher A (1985) Linkage disequilibrium of RFLPs at the beta fibrinogen (FGB) and gamma fibrinogen (FGG) loci on chromosome 4. Cytogenet Cell Genet 40:707–708

Murray JC, Buetow KH, Smith M, Carlock L, Chakravarti A, Ferrell RF, Gedamu L, et al (1988) Pairwise linkage analysis of 11 loci on human chromosome 4. Am J Hum Genet 42:490–497

Murray JC, Demopulos C, Lawn RM, Motulsky AG (1983) Molecular genetics of serum albumin: RFLPs and analbuminemia. Proc Natl Acad Sci USA 80:5951–5955

Murray JC, Shiang R, Carlock LR, Smith M, Buetow KH (1987) Rapid RFLP screening procedure identifies new polymorphisms at albumin and alcohol dehydrogenase loci. Hum Genet 76:274–277

Nakamura Y, Carlson M, Ballard L, O'Connell P, Leppert M, Lathrop GM, Lalouel J-M, White R (1988*a*) Isolation and mapping of a polymorphic DNA sequence (pMCOC14) on chromosome 4p (D4S124). Nucleic Acids Res 16:6254

Nakamura Y, Culver M, O'Connell P, Leppert M, Lathrop GM, Lalouel J-M, White R (1988*b*) Isolation and mapping of a polymorphic DNA sequence (pYNZ32) on chromosome 4p (D4S125). Nucleic Acids Res 16:4186

Pasquinelli C, Garreau F, Bougueleret L, Cariani E, Grzeschik KH, Thiers V, Croissant O, et al. (1988) Rearrangement of a common cellular DNA domain on chromosome 4 in human primary liver tumors. J Virol 62: 629–632

Pohl TM, Zimmer M, MacDonald ME, Smith B, Bucan M, Poustka A, Volinia S, et al. (1988) Construction of a *Not*I linking library and isolation of new markers close to the Huntington's disease gene. Nucleic Acids Res 16:9185–9197

Pritchard CA, Casher D, Uglum E, Cox DR, Myers RM (1989) Isolation and field-inversion gel electrophoresis analysis of DNA markers located close to the Huntington disease gene. Genomics 4:408–418

Richards JE, Gilliam TC, Cole JL, Drumm ML, Wasmuth JJ, Gusella JF, Collins FS (1988) Chromosome jumping from D4S10 (G8) toward the Huntington disease gene. Proc Natl Acad Sci USA 85:6437–6441

Ritty TM, Jaye M, Kaplan R, Murray JC. EcoRIPvuII RFLPs in the endonexin II/annexin V (ANX5) gene on chromosome 4. Nucleic Acids Res (in press)

Ritty TM, Murray JC (1989) A new HincII RFLP for epidermal growth factor (EGF) on chromosome 4. Nucleic Acids Res 17:5870

Royle NJ, Clarkson RE, Wong Z, Jeffreys AJ (1988) Clustering of hypervariable minisatellites in the proterminal regions of human autosomes. Genomics 8:352–360

Scambler PJ, Lord R, Bates G, Williamson R (1985) RFLP for D4S12, an anonymous single copy genomic clone at 4pter-4q26. Nucleic Acids Res 13:3016

Shiang R, Murray JC, Morton CC, Buetow KH, WasmuthJJ, Olney AH, Sanger WG, Goldberger G (1989) Mapping of the human complement factor I gene to 4q25. Genomics 4:1–5

Skraastad MI, Verwest A, de Rooij KE, Vegtervan der Vlis M, Bakker E, Gusella JF, Collins FS, et al (1989) Order of DNA markers near the Huntington locus by multipoint recombination mapping. Cytogenet Cell Genet 51:1081

Smith B, Skarecky D, Bengtsson U, Magenis RE, Carpenter N, Wasmuth JJ (1988) Isolation of DNA markers in the direction of the Huntington disease gene from the G8 locus. Am J Hum Genet 42:335–344

Smith M, Duester G, Carlock L, Wasmuth J (1985) Assignment of ADH1, ADH2, and ADH3 genes (class I ADH) to human chromosome 4q21–4q25 through use of DNA probes. Cytogenet Cell Genet 40:748

Snell RG, Lazarou LP, Youngman S, Quarrell OWJ, Wasmuth JJ, Shaw DJ, Harper PS (1989*a*) Linkage disequilibrium in Huntington's disease: an improved localisation for the gene. J Med Genet 26:673–675

Snell RG, Youngman S, Lehrach H, Sarfarazi M, Harper PS, Shaw DJ (1989*b*) A new probe (2R3) in the region of Huntington's disease. Cytogenet Cell Genet 51:1083

Szauter P (1984) An analysis of regional constraints on exchange in *Drosophila melanogaster* using recombination-defective meiotic mutants. Genetics 106:45–71

Theilmann J, Kanani S, Shiang R, Robbins C, Quarrell O, Huggins M, Hedrick A, et al (1989) Non random association between alleles detected by D4S95 and the Huntington disease gene. J Med Genet 26:676–681

Weber B, Robbins C, Collins C, Theilmann J, Pederson L, Hayden MR (1989) The search for a DNA marker flanking the Huntington's disease gene. Cytogenet Cell Genet 51:1104

Whaley WL, Michiels F, MacDonald ME, Romano D, Zimmer M, Smith B, Leavitt J, et al (1988) Mapping of D4S98/S114/S113 confines the Huntington's defect to a reduced physical region at the telomere of chromosome 4. Nucleic Acids Res 16:11769–11780

Wood S, Starr TV, Shukin RJ (1986) Isolation and characterization of DNA probes from a flow-sorted human chromosome 8 library that detect restriction frgment length polymorphism (RFLP). Am J Hum Genet 39:744–750

Youngman S, Shaw DJ, Gusella JF, MacDonald M, Stanbridge EJ, Wasmuth J, Harper PS (1988) A DNA probe, D5 (D4S90) mapping to human chromosome 4p16.3. Nucleic Acids Res 16:1648